

Non-parametric Reconstruction of Growth Index via Gaussian Processes

Zhao-Yu Yin* and Hao Wei†

School of Physics, Beijing Institute of Technology, Beijing 100081, China

ABSTRACT

The accelerated cosmic expansion could be due to dark energy within general relativity (GR), or modified gravity. It is of interest to differentiate between them, by using both the expansion history and the growth history. In the literature, it was proposed that the growth index γ is useful to distinguish these two scenarios. In this work, we consider the non-parametric reconstruction of the growth index γ as a function of redshift z from the latest observational data as of July 2018 via Gaussian Processes. We find that $f(R)$ theories and dark energy models within GR (especially Λ CDM) are inconsistent with the results in the moderate redshift range far beyond 3σ confidence level. A modified gravity scenario different from $f(R)$ theories is favored. However, these results can also be due to other non-trivial possibilities, in which dark energy models within GR (especially Λ CDM) and $f(R)$ theories might still survive. In all cases, our results suggest that new physics is required.

PACS numbers: 98.80.-k, 98.80.Es, 95.36.+x, 04.50.Kd

* email address: 854587902@qq.com

† Corresponding author; email address: haowei@bit.edu.cn

I. INTRODUCTION

Since the discovery of the accelerated expansion of our universe in 1998 [1, 2], the real cause of this mysterious phenomenon is still unclear so far. As is well known, two main types of scenarios are extensively considered in the literature to this end. The first one is to introduce an unknown component with negative pressure (dark energy) in the framework of general relativity (GR). On the contrary, the second one explains the accelerated expansion by using a modification to GR (modified gravity), without invoking dark energy. We refer to e.g. [3–6] for comprehensive reviews.

Until now, both scenarios are competent to interpret the accelerated cosmic expansion. Therefore, it is of interest to differentiate between them. Since they cannot be distinguished by using the expansion history solely, it is necessary to consider the growth history in addition (see e.g. [7–10] and references therein). In fact, if the models of dark energy and modified gravity share a same expansion history, they might have different growth histories. Typically, the growth history is characterized by the linear matter density contrast $\delta(z) \equiv \delta\rho_m/\rho_m$ as a function of redshift z . It is convenient to introduce the growth rate $f \equiv d\ln\delta/d\ln a$, where $a = (1+z)^{-1}$ is the scale factor. Many years ago, a good approximation $f = \Omega_m^\gamma$ has been first proposed in [11, 12] within GR, where γ is the growth index, and Ω_m is the fractional density of pressureless matter. In the beginning, $f = \Omega_m^\gamma$ was used only at the present time ($z = 0$), and it was not valid for any redshift. Since [13] it was applied to anything beyond matter, curvature, and a cosmological constant. Finally, not until [14] was it applied to gravity other than GR, and then in [7] generalized to modified gravity, varying equation of state, and an integral relation for growth. Nowadays, the general form $f(z) = \Omega_m(z)^{\gamma(z)}$ has been extensively used in the literature.

In e.g. [7, 8], it was proposed that the growth index γ is useful to distinguish the scenarios of dark energy and modified gravity. In GR, $\gamma = 6/11 \simeq 0.545$ for Λ CDM model [7, 8] (which is approximately independent of redshift), while $\gamma \simeq 0.55$ for many dark energy models [7]. In the cases of modified gravity, $\gamma \simeq 0.68$ for Dvali-Gabadadze-Porrati (DGP) model ($\gamma = 11/16$ is its high redshift asymptotic value) [8, 9], while $\gamma \simeq 0.42$ for most of viable $f(R)$ theories ($\gamma \lesssim 0.557$ certainly for almost all viable $f(R)$ theories, and γ decreases when redshift increases) [15–18]. Since their $\gamma(z)$ lie in a narrow range around the above values respectively, one might differentiate between them.

In the literature, the growth indices for some particular models have been constrained by using the observational data, but only the present value γ_0 and the derivative γ'_0 were considered usually. Of course, it is better to study the growth index in a model-independent way. In the literature, a common choice is to consider the model-independent parameterizations for $\gamma(z)$, but a particular function form should be given *a priori*. On the contrary, it is worth noting that the goal function could be directly reconstructed from the input data by using some non-parametric methods, such as principal component analysis, and Gaussian processes, without assuming a particular function form.

Here, we consider the non-parametric reconstruction of the growth index $\gamma(z)$ as a function of redshift z via Gaussian processes [19, 20], by using the latest observational data. In Sec. II, we briefly describe the methodology. In Secs. III and IV, the results and the conclusions are given, respectively. We find that $f(R)$ theories, and dark energy models within GR (especially Λ CDM), are inconsistent with the results in the moderate redshift range, far beyond 3σ confidence level (C.L.). A modified gravity scenario different from $f(R)$ theories is favored. However, there might be other possibilities for these results, and we will discuss this issue briefly in Sec. IV. In all cases, our results suggest that new physics is required.

II. METHODOLOGY

By definition $f(z) = \Omega_m(z)^{\gamma(z)}$, the growth index is given by

$$\gamma(z) = \frac{\ln f(z)}{\ln \Omega_m(z)}. \quad (1)$$

Note that in a few works (e.g. [21, 22]) a fairly different $\gamma(z) = d\ln f(z)/d\ln \Omega_m(z)$ is taken, which coincides with Eq. (1) only when $\gamma = \text{const}$. To reconstruct $\gamma(z)$, both $f(z)$ and $\Omega_m(z)$ are needed.

The growth rate f can be obtained from redshift space distortion (RSD) measurements, and the observational f_{obs} data have been used in some relevant works (e.g. [9, 21, 22]). However, it is sensitive to the bias parameter b which can vary in the range $b \in [1, 3]$. This makes the observational f_{obs} data

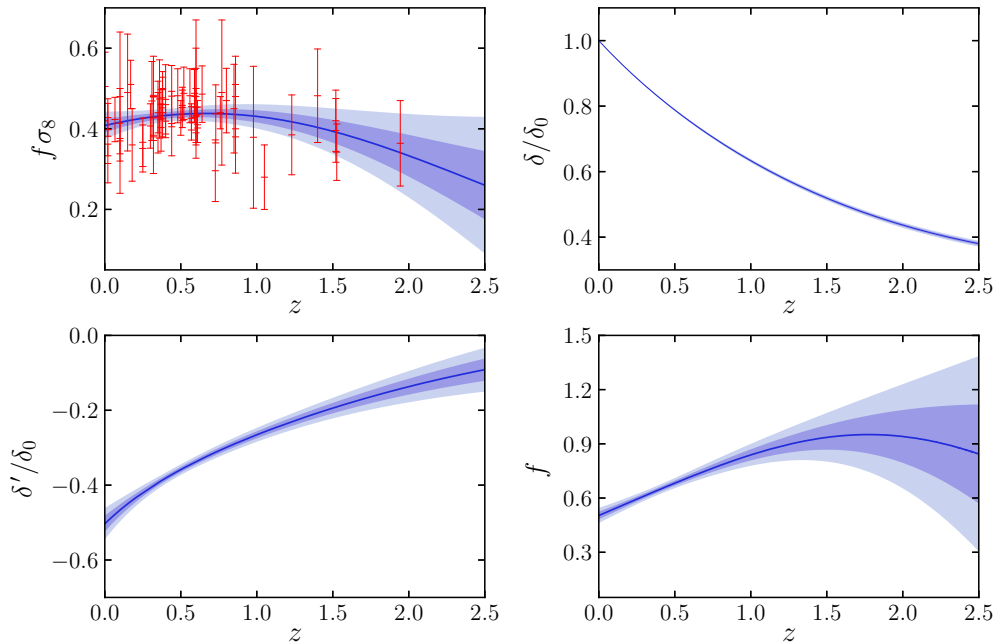


FIG. 1: The reconstructed $f\sigma_8$, δ/δ_0 , δ'/δ_0 and f as functions of redshift z , by using Gaussian processes with the squared exponential covariance function. The mean and 1σ , 2σ uncertainties are indicated by the blue solid lines and the shaded regions, respectively. The observational $f\sigma_{8,obs}$ data with error bars are also plotted in the top-left panel. See the text for details.

unreliable [23]. Instead, the combination $f\sigma_8(z) \equiv f(z)\sigma_8(z)$ is independent of the bias, and hence is more reliable, where $\sigma_8(z) = \sigma_8(z=0)\delta(z)/\delta(z=0) = \sigma_{8,0}\delta(z)/\delta_0$ within spheres of radius $8h^{-1}\text{Mpc}$ [23], and the subscript “0” indicates the present value of the corresponding quantity. Noting that

$$f \equiv \frac{d \ln \delta}{d \ln a} = -(1+z) \frac{\delta'}{\delta}, \quad (2)$$

where a prime denotes the derivative with respect to redshift z , we have

$$\frac{\delta'(z)}{\delta_0} = -\frac{1}{\sigma_{8,0}} \frac{f\sigma_8(z)}{1+z}, \quad (3)$$

$$\frac{\delta(z)}{\delta_0} = 1 - \frac{1}{\sigma_{8,0}} \int_0^z \frac{f\sigma_8(\tilde{z})}{1+\tilde{z}} d\tilde{z}. \quad (4)$$

In fact, the observational $f\sigma_{8,obs}$ data can be obtained from weak lensing and RSD measurements [23, 24]. Once $f\sigma_8(z)$ is reconstructed from the observational $f\sigma_{8,obs}$ data via Gaussian processes [19, 20], we can obtain $\delta'(z)/\delta_0$, $\delta(z)/\delta_0$, and finally $f(z)$ by using Eqs. (3), (4) and (2).

On the other hand, the dimensionless Hubble parameter $E \equiv H/H_0$ is required to reconstruct

$$\Omega_m(z) \equiv \frac{8\pi G\rho_m}{3H^2} = \frac{\Omega_{m0}(1+z)^3}{E^2(z)}. \quad (5)$$

Note that $E(z)$ can also be obtained from the growth history [25–27]. In GR, the perturbation equation $\ddot{\delta} + 2H\dot{\delta} = 4\pi G\rho_m\delta$ can be recast as a differential equation for H^2 , where a dot denotes the derivative with respect to cosmic time t . Its solution is given by [25–27]

$$E^2 = 3\Omega_{m0} \frac{(1+z)^2}{\delta'^2} \int_z^\infty \frac{\delta}{1+\tilde{z}} (-\delta') d\tilde{z}. \quad (6)$$

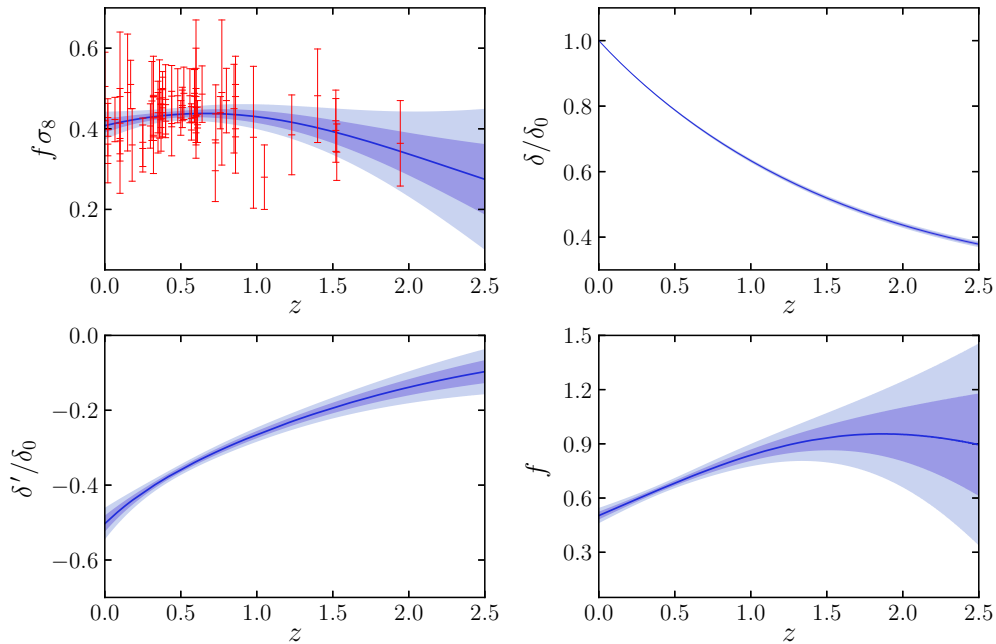


FIG. 2: The same as in Fig. 1, except for the Matérn ($\nu = 9/2$) covariance function. See the text for details.

However, in the case of modified gravity, the perturbation equation becomes $\ddot{\delta} + 2H\dot{\delta} = 4\pi G_{\text{eff}}\rho_m\delta$, and its solution reads [25]

$$E^2 = 3\Omega_{m0} \frac{(1+z)^2}{\delta'^2} \int_z^\infty \frac{-\delta\delta'}{1+\bar{z}} \cdot \frac{G_{\text{eff}}}{G} d\bar{z}, \quad (7)$$

where $G_{\text{eff}} = G(1 + 1/(3\beta))$ is the effective gravitational “constant”, and β depends on time in general, which will be known if the modified gravity is specified. For example, $\beta = -(1 + \Omega_m^2)/(1 - \Omega_m^2)$ for the flat DGP model [9, 10, 25]. Noting Eq. (5), it is difficult to analytically obtain $E(z)$ from Eq. (7) because E^2 appears in the both sides. On the other hand, if we do not know whether GR is modified or not *a priori* (since our goal is to differentiate between dark energy within GR, and modified gravity), we also do not know which one of Eqs. (6) and (7) will be used. Therefore, it is not viable to obtain $E(z)$ by using the growth history.

The only viable way is to use the expansion history. There exist two different approaches to this end. The first one is to directly reconstruct $E(z)$ by using the observational $H(z)$ data [28–30] from the measurements of the differential age and the baryon acoustic oscillation (BAO). The second one is to use the luminosity distance of type Ia supernovae (SNIa), $d_L(z) = (c/H_0)(1+z)D(z)$, where c is the speed of light. Note that we consider a flat Friedmann-Robertson-Walker (FRW) universe throughout. In this case, $D = \int_0^z d\bar{z}/E(\bar{z})$, and hence $E = 1/D'$. Once $E(z)$ is reconstructed from the observational $H(z)$ data or SNIa via Gaussian processes, we can obtain $\Omega_m(z)$ by using Eq. (5). Finally, the growth index $\gamma(z)$ is available from Eq. (1).

We refer to e.g. [19, 20, 31] for the details of Gaussian processes. In this work, we implement Gaussian processes by using the code GaPP (Gaussian Processes in Python) [20]. In Gaussian processes, there are many options for the covariance function (or, the kernel function) $\kappa(z, \bar{z})$. Here, we choose to use two different types of $\kappa(z, \bar{z})$. The first one is the squared exponential (or, Gaussian) covariance function, which is the simplest and popular choice in the literature. The second one is the Matérn ($\nu = 9/2$) covariance function, which is recommended by [31] because it is the best in the ones under consideration. The explicit forms of these two covariance functions can be found in e.g. [19, 20, 27, 31, 32].

Finally, it is of interest to fully extract information from the expansion history. In modified gravity, the modification to GR can also be regarded as an “effective dark energy” component in GR. The equation-of-state parameter (EoS) of the real/effective dark energy is given by $w = -(1/3) d \ln(\Omega_m^{-1} - 1) / d \ln a$ [7].

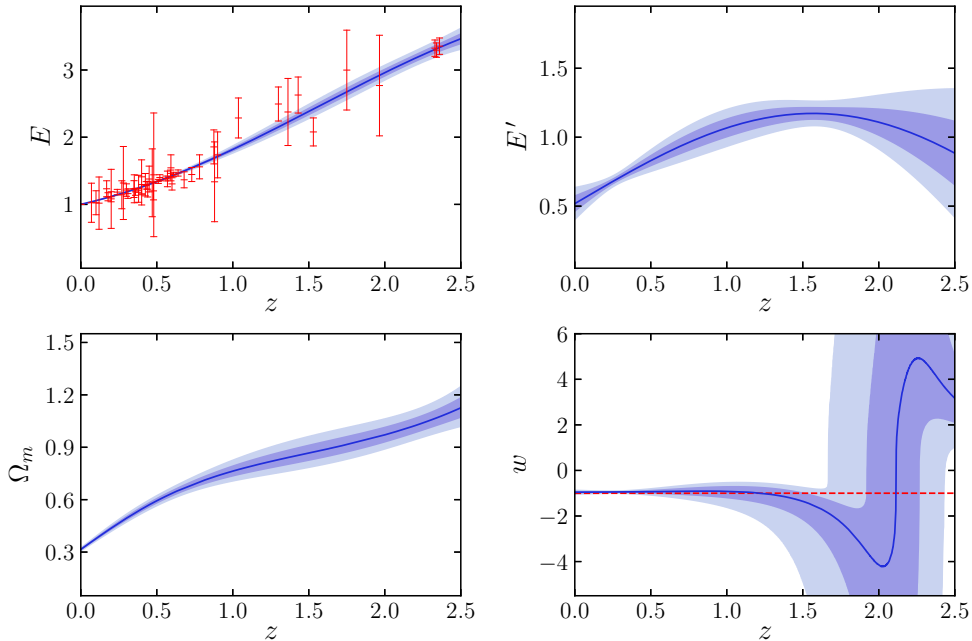


FIG. 3: The reconstructed E , E' , Ω_m and w as functions of redshift z , by using Gaussian processes with the squared exponential covariance function, from the observational $H(z)$ data with $H_0 = 67.36 \pm 0.54$ km/s/Mpc. The mean and 1σ , 2σ uncertainties are indicated by the blue solid lines and the shaded regions, respectively. The observational E_{obs} data with error bars are also plotted in the top-left panel. $w = -1$ is indicated by a red dashed line. See the text for details.

Using Eq. (5) and $E = 1/D'$, it becomes

$$w = \frac{2(1+z)EE' - 3E^2}{3[E^2 - \Omega_{m0}(1+z)^3]} \quad (8)$$

$$= -\frac{2(1+z)D'' + 3D'}{3[D' - \Omega_{m0}(1+z)^3D'^3]}. \quad (9)$$

So, $w(z)$ can also be reconstructed from the observational $H(z)$ data or SNIa via Gaussian processes.

III. RESULTS

In the following, we use the latest observational data as of July 2018. We first reconstruct $f(z)$ via Gaussian processes. In [24], a sample consisting of 63 observational $f\sigma_8, obs$ data published to date are given, which is the largest $f\sigma_8$ compilation in the literature by now. We can reconstruct $f\sigma_8(z)$ from the observational data, and then δ'/δ_0 , δ/δ_0 and f from Eqs. (3), (4) and (2), respectively. Note that in Eqs. (3) and (4), we adopt $\sigma_{8,0} = 0.8111 \pm 0.0060$ from the newest Planck 2018 results [33, 34]. The reconstructed $f\sigma_8$, δ/δ_0 , δ'/δ_0 and f as functions of redshift z are given in Figs. 1 and 2. Clearly, the choices of covariance function only make fairly small difference.

Then, we reconstruct $\Omega_m(z)$ while $E(z) = H(z)/H_0$ in it can be reconstructed by using the expansion history. As mentioned above, two ways are viable. At first, we consider the 51 observational $H(z)$ data compiled in [28], which is the largest sample by now to our best knowledge. Here, the Hubble constant H_0 is required to convert the observational $H(z)$ data into the observational $E(z)$ data. As is well known, two observational H_0 values from the observations at high and low redshifts are in significant tension. The newest $H_0 = 67.36 \pm 0.54$ km/s/Mpc from the Planck 2018 results [33, 34] is much smaller than the newest $H_0 = 73.52 \pm 1.62$ km/s/Mpc from the SH0ES 2018 results [35], beyond 3.6σ C.L. Since the debate is not settled by now, we choose to use them equally. The uncertainties in the observational $H(z)$ data

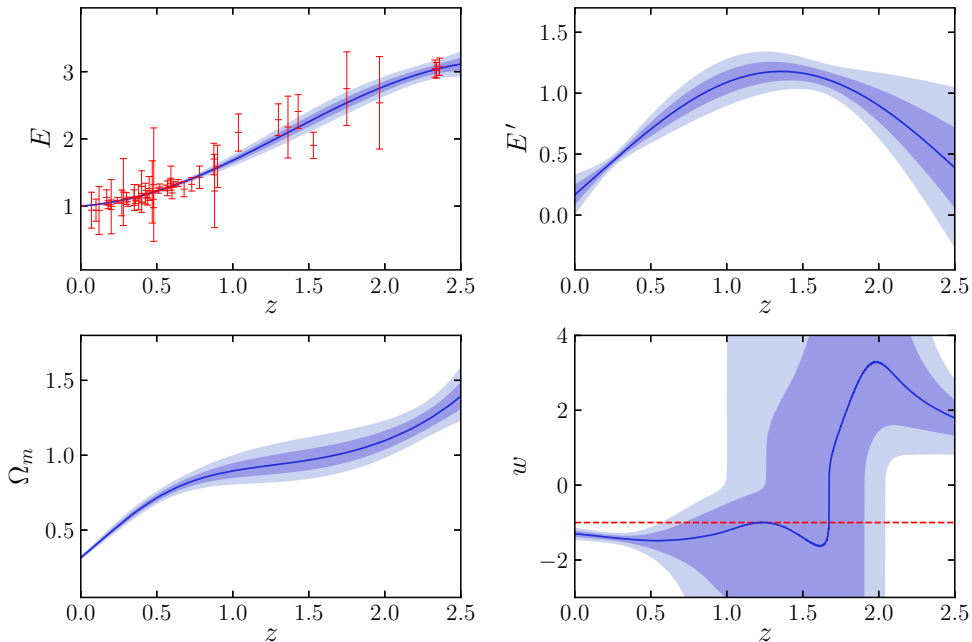


FIG. 4: The same as in Fig. 3, except for the squared exponential covariance function, and $H_0 = 73.52 \pm 1.62$ km/s/Mpc. See the text for details.

and H_0 are propagated to the E_{obs} data analytically [36, 37], through $\sigma_E^2 = \sigma_H^2/H_0^2 + (H^2/H_0^4)\sigma_{H_0}^2$ [38]. On the other hand, $E(z=0) = 1$ exactly by definition. We can reconstruct $E(z)$ and $E'(z)$ from the observational E_{obs} data via Gaussian processes, and then Ω_m and w from Eqs. (5) and (8), in which we adopt $\Omega_{m0} = 0.3153 \pm 0.0073$ from the newest Planck 2018 results [33, 34]. The reconstructed E , E' , Ω_m and w as functions of redshift z are given in Figs. 3~6. Clearly, the choices of covariance function only make fairly small difference, but the choices of H_0 make considerable difference. In particular, $w = -1$ is fully consistent with the reconstructed $w(z)$ in the cases of $H_0 = 67.36 \pm 0.54$ km/s/Mpc, but $w < -1$ is slightly favored in the cases of $H_0 = 73.52 \pm 1.62$ km/s/Mpc.

As an alternative, we can also reconstruct $E = 1/D'$ from the luminosity distance of SNIa. Here we use the Pantheon sample [39–41] consisting of 1048 SNIa, which is the largest spectroscopically confirmed SNIa sample by now. The corrected bolometric apparent magnitude m is related to D according to [42]

$$m = 5 \log_{10}((1+z)D) + \mathcal{M}, \quad (10)$$

where \mathcal{M} is a nuisance parameter representing some combination of the absolute magnitude M and H_0 . One can convert the observational m data given in the Pantheon plugin [41] into the D_{obs} data, while their covariance matrices are related by the propagation of uncertainty [43], $\mathbf{C}_D = \mathbf{J}\mathbf{C}_m\mathbf{J}^T$, where \mathbf{J} is the Jacobian matrix. Note that we consider the full covariance matrix with the systematic uncertainties. Here we adopt the best-fit $\mathcal{M} = 23.808891$ for the flat Λ CDM model [42] as a fiducial value. We can reconstruct $D(z)$, $D'(z)$ and $D''(z)$ from the observational D_{obs} data via Gaussian processes, and then $E = 1/D'$, as well as Ω_m and w from Eqs. (5) and (9), in which we adopt again $\Omega_{m0} = 0.3153 \pm 0.0073$ from the newest Planck 2018 results [33, 34]. The reconstructed D , D' , D'' , E , Ω_m and w as functions of redshift z are given in Figs. 7 and 8. Clearly, the choices of covariance function only make fairly small difference. In both cases, $w = -1$ is fully consistent with the reconstructed $w(z)$.

Finally, using the above reconstructed $f(z)$ and $\Omega_m(z)$, we obtain the growth index γ as a function of redshift z from Eq. (1). We present the reconstructed $\gamma(z)$ in Fig. 9, for various observational data and Gaussian processes with different covariance functions. It is easy to see that the choices of covariance function only make fairly small difference. Notably, $\gamma \simeq 0.42$ ($f(R)$ theories) [15–18] is inconsistent with the reconstructed $\gamma(z)$ in the redshift range $0 \leq z \lesssim 0.8$ far beyond 3σ C.L. in all cases (see Fig. 9). Also, $\gamma_0 \simeq 0.42$ at $z = 0$ is strongly disfavored at very high C.L. On the other hand, also in all cases,

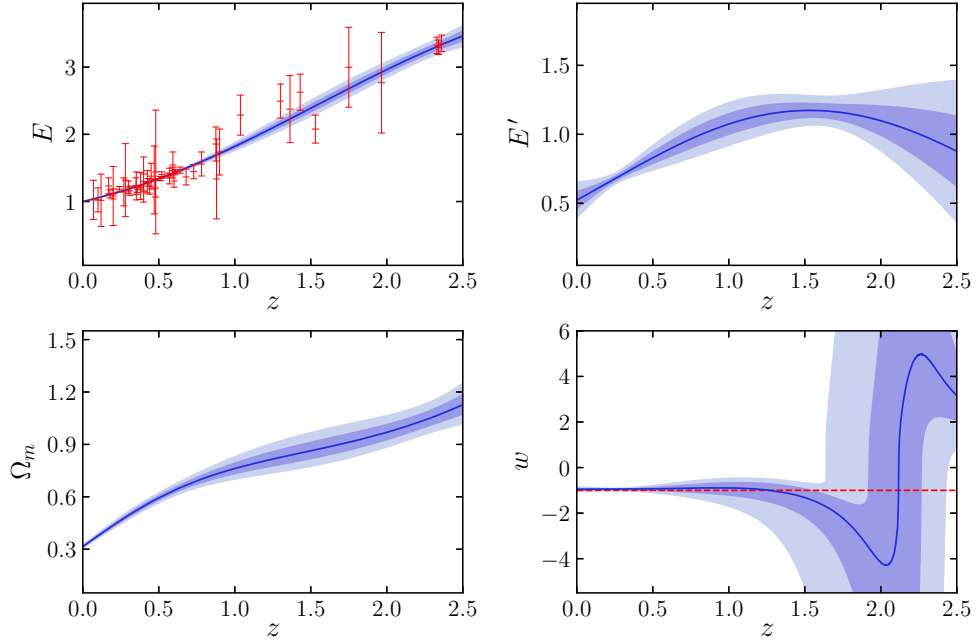


FIG. 5: The same as in Fig. 3, except for the Matérn ($\nu = 9/2$) covariance function, and $H_0 = 67.36 \pm 0.54$ km/s/Mpc. See the text for details.

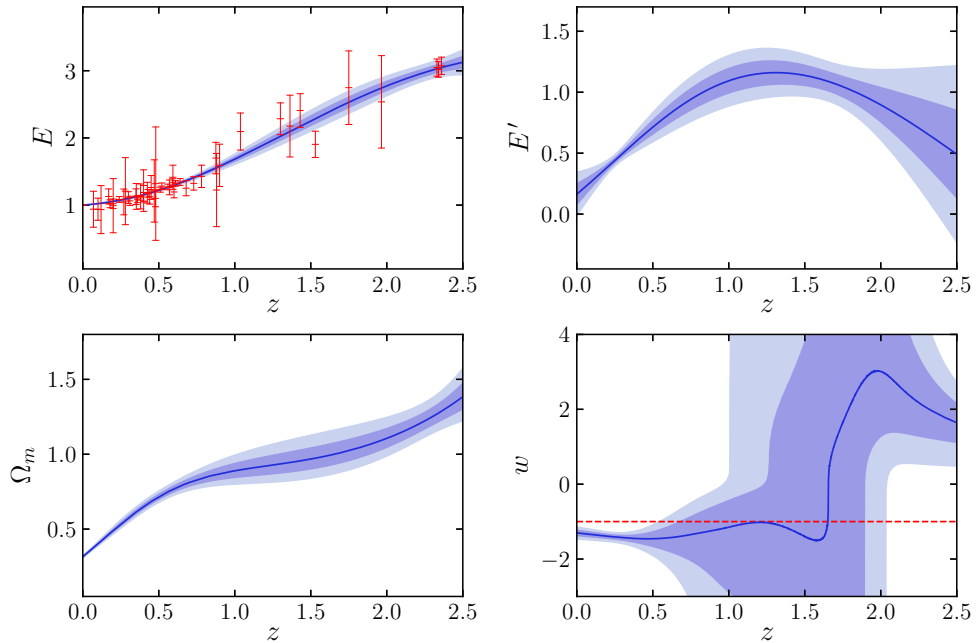


FIG. 6: The same as in Fig. 3, except for the Matérn ($\nu = 9/2$) covariance function, and $H_0 = 73.52 \pm 1.62$ km/s/Mpc. See the text for details.

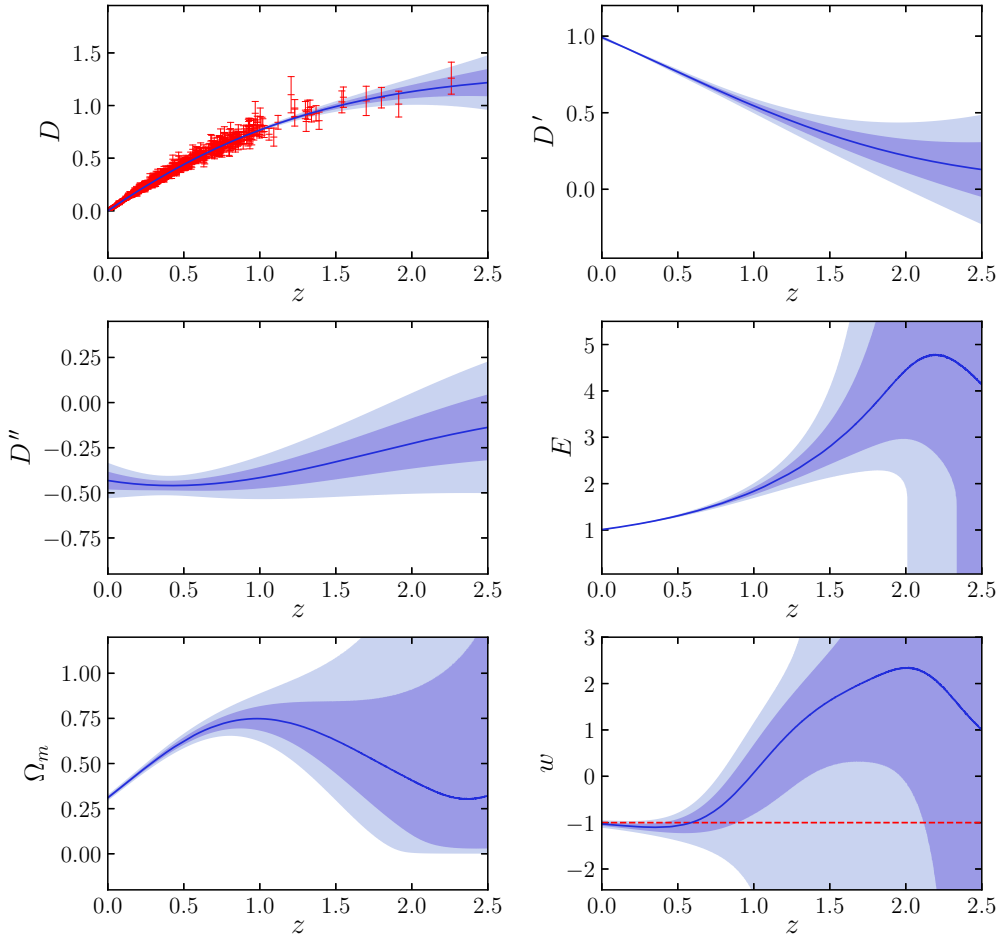


FIG. 7: The reconstructed D , D' , D'' , E , Ω_m and w as functions of redshift z , by using Gaussian processes with the squared exponential covariance function, from the Pantheon SNIa data. The mean and 1σ , 2σ uncertainties are indicated by the blue solid lines and the shaded regions, respectively. The observational D_{obs} data with error bars are also plotted in the top-left panel. $w = -1$ is indicated by a red dashed line. See the text for details.

although $\gamma_0 \simeq 0.55$ at $z = 0$ and $\gamma \simeq 0.55$ (dark energy models within GR) [7] at low redshift $z \lesssim 0.1$ are consistent with the results, from Fig. 9 one can see that $\gamma \simeq 0.55$ is still inconsistent with the reconstructed $\gamma(z)$ in the moderate redshift range $0.1 \lesssim z \lesssim 0.7$ far beyond 3σ C.L., due to the arched structure in the reconstructed $\gamma(z)$. In particular, for Λ CDM model $\gamma = 6/11 \simeq 0.545$ [7, 8], which is approximately independent of redshift. Therefore, it is also disfavored far beyond 3σ C.L. At last, the status is fairly subtle for $\gamma \simeq 0.68$ (DGP model) [8, 9]. From Fig. 9, we find that in the cases of the observational $H(z)$ data with $H_0 = 67.36 \pm 0.54$ km/s/Mpc and the Pantheon SNIa data, $\gamma \simeq 0.68$ is fully consistent with the reconstructed $\gamma(z)$. However, in the case of the observational $H(z)$ data with $H_0 = 73.52 \pm 1.62$ km/s/Mpc, $\gamma \simeq 0.68$ is inconsistent with the results in the moderate redshift range (see the middle panels of Fig. 9), due to the arched structure in the reconstructed $\gamma(z)$. Since the tension between the above two H_0 is beyond 3.6σ , and the debate in the community is not settled by now, we can say nothing certainly about $\gamma \simeq 0.68$ (DGP model) so far.

Nevertheless, our results strongly suggest that the growth index $\gamma(z)$ is varying. The arched structure in the reconstructed $\gamma(z)$ shown in Fig. 9 plays an important role. The derivative $\gamma' > 0$ at low redshift, and $\gamma' < 0$ at higher redshift. The models with $\gamma \lesssim 0.55$ in the moderate redshift range $0.1 \lesssim z \lesssim 0.7$ are disfavored far beyond 3σ C.L.

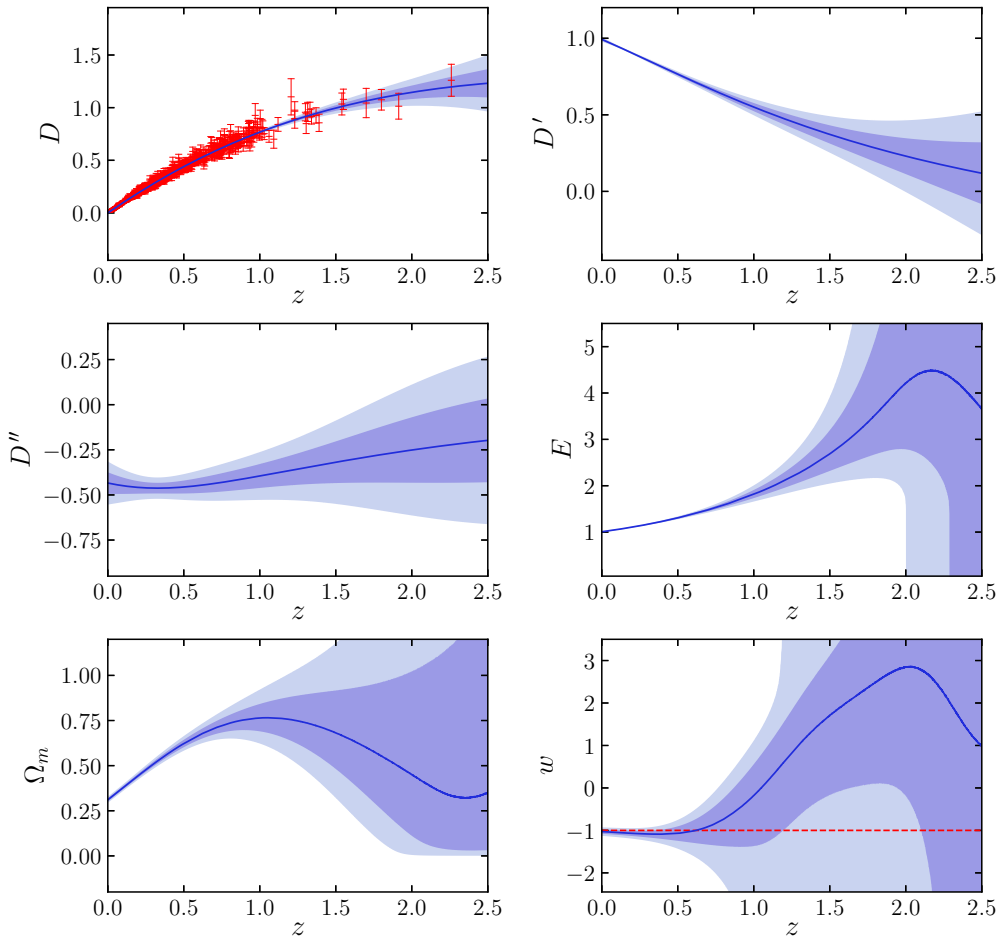


FIG. 8: The same as in Fig. 7, except for the Matérn ($\nu = 9/2$) covariance function. See the text for details.

IV. CONCLUSION AND DISCUSSION

The accelerated cosmic expansion could be due to dark energy within GR, or modified gravity. It is of interest to differentiate between them, by using both the expansion history and the growth history. In the literature, it was proposed that the growth index γ is useful to distinguish these two scenarios. In this work, we consider the non-parametric reconstruction of the growth index γ as a function of redshift z from the latest observational data as of July 2018 via Gaussian Processes. Interestingly, we find that $f(R)$ theories and dark energy models within GR (especially Λ CDM) are inconsistent with the results in the moderate redshift range far beyond 3σ C.L., due to the arched structure in the reconstructed $\gamma(z)$. A modified gravity scenario different from $f(R)$ theories is favored.

Obviously, this result is unusual, and new physics is required. However, it does not mean that dark energy models within GR (especially Λ CDM) and $f(R)$ theories certainly end. First, one can doubt the observational data used in this work. For instance, the 63 observational $f\sigma_8, obs$ data compiled in [24] might be correlated, and contain duplicated points from the same surveys, while the corrections from the choices of the fiducial cosmology should be taken into account. So, this $f\sigma_8, obs$ sample might require a re-analysis, as preliminarily considered in [23, 24]. Second, the reliability of Gaussian Processes at high redshift might be questionable. Therefore, we should test the growth index γ by using another independent method, and cross-check the corresponding results with the ones from Gaussian Processes. In fact, our relevant work will appear in a separate paper [46]. Finally, in the present work, cold dark

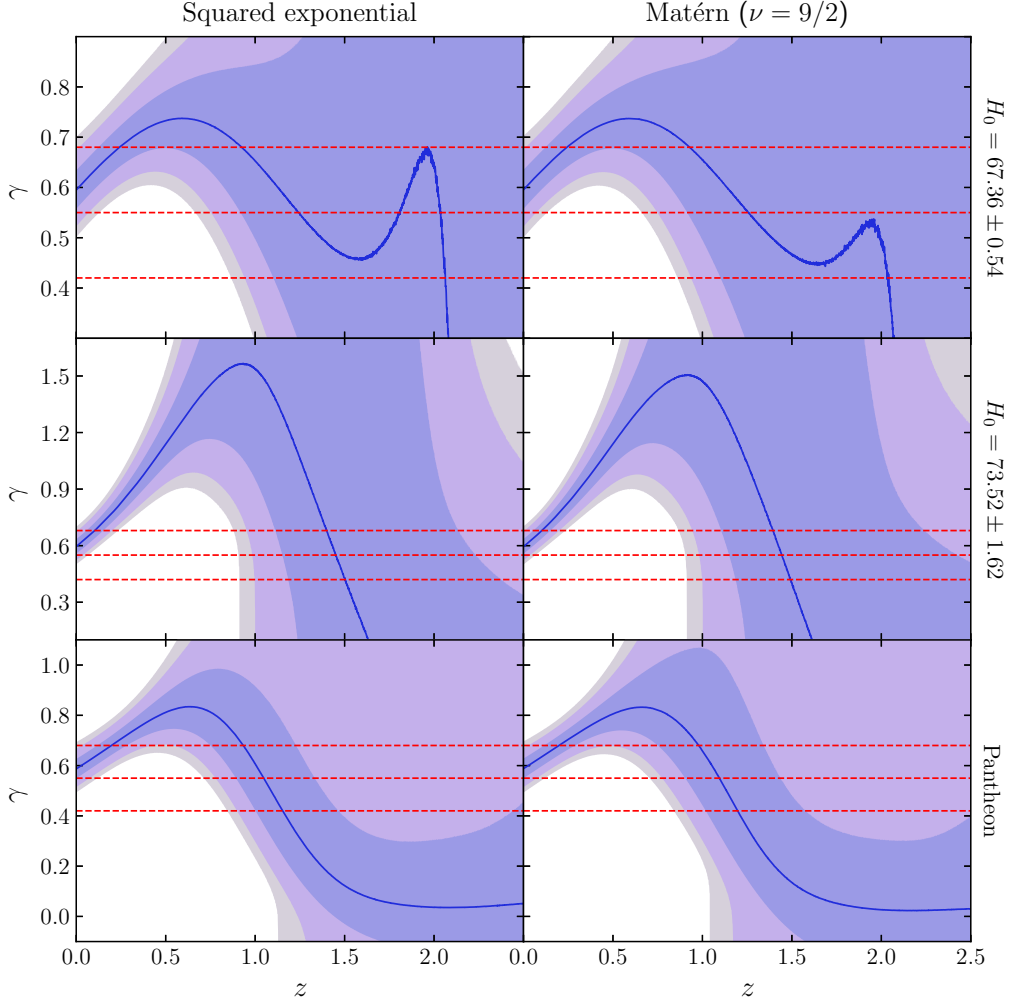


FIG. 9: The reconstructed growth index γ as a function of redshift z , by using the latest observational data via Gaussian processes. The mean and 1σ , 2σ , 3σ uncertainties are indicated by the blue solid lines and the shaded regions, respectively. The left and right panels correspond to the squared exponential and the Matérn ($\nu = 9/2$) covariance functions, respectively. The top, middle, and bottom panels correspond to the observational $H(z)$ data with $H_0 = 67.36 \pm 0.54$ km/s/Mpc, $H_0 = 73.52 \pm 1.62$ km/s/Mpc, and the Pantheon SNIa data, respectively. $\gamma = 0.42$ ($f(R)$ theories), 0.55 (dark energy models in GR, especially Λ CDM), 0.68 (DGP model) are indicated by the red dashed lines. See the text for details.

matter is implicitly assumed, as in Eq. (5). If there is a non-zero interaction between dark energy and dark matter, Eq. (5) should be changed to

$$\Omega_m(z) \equiv \frac{8\pi G\rho_m}{3H^2} = \frac{\Omega_{m0}(1+z)^{3+\xi}}{E^2(z)}, \quad (11)$$

where ξ characterizes the deviation from uncoupled cold dark matter (note that ξ can be time-dependent in general). Another non-trivial possibility assumes that dark matter is not cold. In fact, for warm dark matter, its equation-of-state parameter $w_m \neq 0$, and hence $\Omega_m(z)$ takes a form similar to Eq. (11). In both non-trivial cases, the conclusions should be changed, and dark energy models within GR (especially Λ CDM) and $f(R)$ theories might still survive (see [10, 47] for deeper discussions). The new physics in these non-trivial cases lies in the non-zero interaction between dark energy and dark matter, or the induction of warm dark matter. They deserve further investigations.

After all, we would like to mention several technical details. One might note that in Figs. 3~6 the reconstructed Ω_m becomes larger than 1 at high redshift $z \gtrsim 2$, but this is not unphysical in fact. Yes, in GR, the Friedmann equation $H^2 = 8\pi G(\rho_m + \rho_X)/3$ is unchanged, and hence $0 \leq \Omega_m \leq 1$ by definition. However, this is right only for dark energy models in GR. On the contrary, in modified gravity, the Friedmann equation should be modified, and the modification to GR can be equivalent to an effective “energy component”. So, the effective ρ_X can be negative at high redshift, and hence $\Omega_m > 1$ is possible. Since the effective “energy component” is not real matter (it is actually the modification to GR, namely a geometric effect indeed), this is allowed by physics. In fact, noting that $0 \leq \Omega_m \leq 1$ must be held for dark energy models in GR, our reconstructed $\Omega_m > 1$ at high redshift $z \gtrsim 2$ in Figs. 3~6 can be regarded as an extra evidence supporting modified gravity against dark energy models in GR.

It is known that in modified gravity, e.g. $f(R)$ theories, the growth rate $f = f(z, k)$ is also spatially scale-dependent in general (see e.g. [15, 16, 44]), where the comoving wavenumber k denotes the scale [45]. In principle, the scale-dependence should be taken into account (we thank the referee for pointing out this issue). However, let us have a closer look. In [15], they found that f and hence γ is scale-independent at redshift $z \lesssim 0.5$ (see their Fig. 2 and the text below Eq. (4.17) or Eq. (58) in the arXiv version). At $z = 0$, they found $\gamma_0 \simeq 0.41$ independent of the scales k . At higher redshift, they have a small difference $\Delta\gamma \lesssim 0.04$ between various scales. γ becomes smaller as redshift z increases, so that $\gamma \lesssim 0.41$ at higher redshift. In [16], the results are quite similar. They found that the dispersion of γ with respect to the scale k is very small (see their Fig. 2 and the text in Sec. IV.B), namely γ is nearly scale-independent at redshift $z \lesssim 1$ (especially the dispersion of γ is nearly absent for scales $k \geq 0.033h \text{ Mpc}^{-1}$). Again, γ becomes smaller as redshift z increases. On the other hand, from their Figs. 1, 3, 4, 6, 7, one can see that $\gamma_0 = \gamma(z = 0)$ is smaller than ~ 0.557 for various model parameters of viable $f(R)$ theories, and this is independent of the scales k . Keeping the above results of [15, 16] in mind, let us turn back to our Fig. 9. First, in all cases of Fig. 9, $\gamma_0 \lesssim 0.5$ at $z = 0$ is clearly inconsistent with our reconstructed $\gamma(z)$ beyond 3σ C.L. As mentioned above, it is found in [15, 16] that $\gamma_0 = \gamma(z = 0)$ is smaller than ~ 0.557 for various model parameters of viable $f(R)$ theories, and this is independent of the scales k . So, our results of γ_0 is a bad news to most of these viable $f(R)$ theories, although it is not so decisive. Second, in all cases of Fig. 9, $\gamma < 0.56$ in the moderate redshift range $0.1 \lesssim z \lesssim 0.7$ is also clearly inconsistent with our reconstructed $\gamma(z)$ far beyond 3σ C.L. Actually, in all cases of Fig. 9, even $\gamma \lesssim 0.6$ is still inconsistent with our reconstructed $\gamma(z)$ beyond 3σ C.L. in a relatively narrower moderate redshift range. As mentioned above, it is found in [15, 16] that γ becomes smaller as redshift z increases. Together with the fact that $\gamma_0 = \gamma(z = 0)$ is smaller than ~ 0.557 for various model parameters of viable $f(R)$ theories, it is easy to see that $\gamma \lesssim 0.557 < 0.56$ in the moderate redshift range $0.1 \lesssim z \lesssim 0.7$. This is also independent of the scales k . Note that we can further relax 0.56 to the larger 0.6 as mentioned above. Therefore, we can still say that most of viable $f(R)$ theories with various model parameters are inconsistent with our reconstructed $\gamma(z)$ in the moderate redshift range beyond 3σ C.L., and this conclusion is nearly scale-independent actually. Finally, even in the worst case that our results are not applicable to $f(R)$ theories due to the scale-dependence, our other conclusion that dark energy models in GR (especially Λ CDM) are inconsistent with our reconstructed $\gamma(z)$ in the moderate redshift range far beyond 3σ C.L. is still valid. New physics is still required.

ACKNOWLEDGEMENTS

We thank the anonymous referee for useful comments and suggestions, which helped us to improve this work. We are grateful to Hua-Kai Deng, Xiao-Bo Zou, Da-Chun Qiang, Zhong-Xi Yu, and Shou-Long Li for kind help and discussions. This work was supported in part by NSFC under Grants No. 11575022 and No. 11175016.

-
- [1] A. G. Riess *et al.*, *Astron. J.* **116**, 1009 (1998) [astro-ph/9805201].
 - [2] S. Perlmutter *et al.*, *Astrophys. J.* **517**, 565 (1999) [astro-ph/9812133].
 - [3] M. Ishak, *Living Rev. Rel.* **22**, no. 1, 1 (2019) [arXiv:1806.10122].

- [4] L. Amendola *et al.*, Living Rev. Rel. **21**, no. 1, 2 (2018) [arXiv:1606.00180].
- [5] A. Joyce, B. Jain, J. Khoury and M. Trodden, Phys. Rept. **568**, 1 (2015) [arXiv:1407.0059].
- [6] T. Clifton, P. G. Ferreira, A. Padilla and C. Skordis, Phys. Rept. **513**, 1 (2012) [arXiv:1106.2476].
- [7] E. V. Linder, Phys. Rev. D **72**, 043529 (2005) [astro-ph/0507263].
- [8] E. V. Linder and R. N. Cahn, Astropart. Phys. **28**, 481 (2007) [astro-ph/0701317].
- [9] H. Wei, Phys. Lett. B **664**, 1 (2008) [arXiv:0802.4122].
- [10] H. Wei and S. N. Zhang, Phys. Rev. D **78**, 023011 (2008) [arXiv:0803.3292].
- [11] P. J. E. Peebles, *Large-Scale Structure of the Universe*, Princeton University Press (1980);
P. J. E. Peebles, *Astrophys. J.* **284**, 439 (1984).
- [12] O. Lahav, P. B. Lilje, J. R. Primack and M. J. Rees, Mon. Not. Roy. Astron. Soc. **251**, 128 (1991).
- [13] L. M. Wang and P. J. Steinhardt, *Astrophys. J.* **508**, 483 (1998) [astro-ph/9804015].
- [14] A. Lue, R. Scoccimarro and G. D. Starkman, Phys. Rev. D **69**, 124015 (2004) [astro-ph/0401515].
- [15] R. Gannouji, B. Moraes and D. Polarski, JCAP **0902**, 034 (2009) [arXiv:0809.3374].
- [16] S. Tsujikawa *et al.*, Phys. Rev. D **80**, 084044 (2009) [arXiv:0908.2669].
- [17] A. Shafieloo, A. G. Kim and E. V. Linder, Phys. Rev. D **87**, no. 2, 023520 (2013) [arXiv:1211.6128].
- [18] S. Tsujikawa, Lect. Notes Phys. **800**, 99 (2010) [arXiv:1101.0191].
- [19] C. E. Rasmussen and C. K. I. Williams, *Gaussian Processes for Machine Learning*, MIT Press (2006).
- [20] M. Seikel, C. Clarkson and M. Smith, JCAP **1206**, 036 (2012) [arXiv:1204.2832];
The code GaPP is publicly available at <http://www.acgc.uct.ac.za/~seikel/GAPP/index.html>
- [21] J. E. Gonzalez, J. S. Alcaniz and J. C. Carvalho, JCAP **1604**, 016 (2016) [arXiv:1602.01015].
- [22] J. E. Gonzalez, J. S. Alcaniz and J. C. Carvalho, JCAP **1708**, 008 (2017) [arXiv:1702.02923].
- [23] S. Nesseris, G. Pantazis and L. Perivolaropoulos, Phys. Rev. D **96**, 023542 (2017) [arXiv:1703.10538].
- [24] L. Kazantzidis and L. Perivolaropoulos, Phys. Rev. D **97**, 103503 (2018) [arXiv:1803.01337].
- [25] T. Chiba and R. Takahashi, Phys. Rev. D **75**, 101301 (2007) [astro-ph/0703347].
- [26] A. A. Starobinsky, JETP Lett. **68**, 757 (1998) [astro-ph/9810431].
- [27] M. J. Zhang and H. Li, Eur. Phys. J. C **78**, no. 6, 460 (2018) [arXiv:1806.02981].
- [28] J. Magana *et al.*, Mon. Not. Roy. Astron. Soc. **476**, no. 1, 1036 (2018) [arXiv:1706.09848].
- [29] J. J. Geng *et al.*, Commun. Theor. Phys. **70**, no. 4, 445 (2018) [arXiv:1806.10735].
- [30] H. Wei and S. N. Zhang, Phys. Lett. B **644**, 7 (2007) [astro-ph/0609597];
H. Wei and S. N. Zhang, Phys. Lett. B **654**, 139 (2007) [arXiv:0704.3330].
- [31] M. Seikel and C. Clarkson, arXiv:1311.6678 [astro-ph.CO].
- [32] R. G. Cai and T. Yang, Phys. Rev. D **95**, no. 4, 044024 (2017) [arXiv:1608.08008];
T. Yang, Z. K. Guo and R. G. Cai, Phys. Rev. D **91**, no. 12, 123533 (2015) [arXiv:1505.04443].
- [33] N. Aghanim *et al.* [Planck Collaboration], arXiv:1807.06209 [astro-ph.CO].
- [34] Y. Akrami *et al.* [Planck Collaboration], arXiv:1807.06205 [astro-ph.CO].
- [35] A. G. Riess *et al.*, *Astrophys. J.* **861**, no. 2, 126 (2018) [arXiv:1804.10655].
- [36] U. Alam, V. Sahni, T. D. Saini and A. A. Starobinsky, astro-ph/0406672.
- [37] H. Wei, N. N. Tang and S. N. Zhang, Phys. Rev. D **75**, 043009 (2007) [astro-ph/0612746].
- [38] M. Seikel, S. Yahya, R. Maartens and C. Clarkson, Phys. Rev. D **86**, 083001 (2012) [arXiv:1205.3431].
- [39] D. M. Scolnic *et al.*, *Astrophys. J.* **859**, no. 2, 101 (2018) [arXiv:1710.00845].
- [40] The numerical data of the full Pantheon SNIa sample are available at
<http://dx.doi.org/10.17909/T95Q4X>
<https://archive.stsci.edu/prepds/ps1cosmo/index.html>
- [41] The Pantheon plugin for CosmoMC is available at
<https://github.com/dscolnic/Pantheon>
- [42] H. K. Deng and H. Wei, Eur. Phys. J. C **78**, no. 9, 755 (2018) [arXiv:1806.02773].
- [43] https://en.wikipedia.org/wiki/Propagation_of_uncertainty
- [44] E. Jennings *et al.*, Mon. Not. Roy. Astron. Soc. **425**, 2128 (2012) [arXiv:1205.2698].
- [45] S. Tsujikawa, Phys. Rev. D **76**, 023514 (2007) [arXiv:0705.1032].
- [46] Z. Y. Yin and H. Wei, arXiv:1902.00289 [astro-ph.CO].
- [47] H. Wei, J. Liu, Z. C. Chen and X. P. Yan, Phys. Rev. D **88**, 043510 (2013) [arXiv:1306.1364].